Dissecting the Cofactor-Dependent and Independent Bindings of PDE4 Inhibitors

Susana Liu, France Laliberté, Brian Bobechko, Adrienne Bartlett, Paula Lario, Elise Gorseth, Jonathan Van Hamme, Michael J. Gresser, and Zheng Huang*

Department of Biochemistry and Molecular Biology, Merck Frosst Center for Therapeutical Research, P.O. Box 1005, Pointe Claire, Dorval, Quebec H9R 4P8, Canada

Received January 16, 2001; Revised Manuscript Received June 20, 2001

ABSTRACT: Type 4 phosphodiesterases (PDE4s) are metallohydrolases that catalyze the hydrolysis of cAMP to AMP. At the bottom of its active site lie two divalent metal ions in a binuclear motif which are involved in both cAMP binding and catalysis [(2000) *Science 288*, 1822−1825; (2000) *Biochemistry 39*, 6449−6458]. Using a SPA-based equilibrium [^{3}H]rolipram binding assay, we have determined that Mg^{2+}, Mn^{2+}, and Co^{2+} all mediated a high-affinity (K_d between 3 and 8 nM) and near stoichiometric (*R*)-rolipram binding to PDE4. In their absence, (*R*)-rolipram binds stoichiometrically to the metal ion-free apoenzyme with a K_d of ∼150 nM. The divalent cation dose responses in mediating the high-affinity rolipram/PDE4 interaction mirror their efficacy in catalysis, suggesting that both metal ions of the holoenzyme are involved in mediating the high-affinity (*R*)-rolipram/PDE4 interaction. The specific rolipram binding to the apo- and holoenzyme is differentially displaced by cAMP, AMP, and other inhibitors, providing a robust tool to dissect the components of metal ion-dependent and independent PDE4/ligand interactions. cAMP binds to the holoenzyme with a K_s of 1.9 μM and nonproductively to the apoenzyme with a K_d of 179 μM. In comparison, AMP binds to the holo- and apoenzyme with K_d values of 7 and 11 mM, respectively. The diminished Mg^{2+}-dependent component of AMP binding to PDE4 suggests that most of the Mg^{2+}/phosphate interaction in the cAMP/PDE4 complex is disrupted upon the hydrolysis of the cyclic phosphoester bond, leading to the rapid release of AMP.

Cyclic nucleotide phosphodiesterases (PDEs)[1] are divalent cation-dependent hydrolases involved in the hydrolysis of cAMP and cGMP, the second messengers responsible for transducing the signals of a variety of extracellular mediators. In concert with multiple adenylate cyclases, 11 families of PDEs, which share a conserved catalytic domain (∼270 amino acids), are involved in regulating the cAMP- and cGMP-mediated signaling processes in specific tissues and subcellular locations (*1*, *2*). The type 4 phosphodiesterases (PDE4s), encoded by four distinct genes (4A, 4B, 4C, and 4D), are the predominant enzymes responsible for the metabolism of cAMP in proinflammatory and immune cells. Multiple gene products exist for each of the four isoforms due to the activation of intronic promoters and/or alternative mRNA splicing, giving rise to variants within each isoform sharing identical catalytic and C-terminal domains. Their divergent N-terminals contain signals for compartmentalization and protein/protein interactions, allowing the regulation of cAMP levels in discrete subcellular locations to fine-tune the cAMP-dependent response (*3*). Gene deletion studies suggest that each isoform plays a nonredundant role in cAMP signaling. Mice lacking the PDE4D isoform, which have approximately 40% reduced PDE4 activity in brain, exhibited delayed growth, reduced fertility, and compromised cholinergic responses (*4*, *5*).

The activity of PDE4, like other PDEs, requires the presence of a divalent cation cofactor such as Mg^{2+}, Mn^{2+}, Zn^{2+}, or Co^{2+}, and Mg^{2+} has been proposed to be the endogenous cofactor (*6*−*10*). Using a fluorescence resonance energy transfer (FRET) based binding assay, we have determined that the binding of Mg^{2+} to PDE4 is responsible for eliciting its high affinity ($K_s \sim 1.9$ μM) interaction with cAMP and activating the catalytic machinery (*7*). The crystal structure of PDE4B identified the presence of two divalent cations bound to residues absolutely conserved among all PDEs (*11*). The two ions are arranged as a binuclear ion motif at the bottom of its deep active site similar to that in DNA polymerase (*12*). One of them (M_1) coordinates to the conserved His^{238}, His^{274}, Asp^{275}, and Asp^{392} while the second (M_2) is loosely bound to Asp^{275} and M_1 via a hydroxide in the absence of cAMP (see Figure 8 for details). A docking study suggests that the binuclear center is in position to coordinate with the phosphoryl oxygens of cAMP to (a) enhance cAMP binding, (b) increase the phosphate electrophilicity, and (c) provide an activated hydroxide nucleophile for hydrolyzing the phosphoester bond (*7*, *11*).

PDE4 inhibitors represent promising agents for managing various diseases including asthma and chronic obstructive pulmonary disease (COPD) (*13*−*15*). In addition to having

* To whom correspondence should be addressed. Fax: (514) 428-4900. Tel: (514) 428-3143. E-mail: zheng_huang@merck.com.

[1] Abbreviations: cAMP, 3′,5′-cyclic adenosine monophosphate; CDP-840, (*R*)-(+)-4-[2-(3-cyclopentyloxy-4-methoxyphenyl)-2-phenylethyl]pyridine; CPMs, scintillation counts per minute; GST, glutathione *S*-transferase; IBMX, 3-isobutyl-1-methylxanthine; FRET, fluorescence resonance energy transfer; PDE, 3′,5′-cyclic nucleotide phosphodiesterase; PDE4, type 4 phosphodiesterase; PMNPQ, 6-(4-pyridylmethyl)-8-(3-nitrophenyl)quinoline; Rolipram, 4-[3-(cyclopentyloxy)-4-methoxyphenyl]-2-pyrrolidinone; Ariflo (SB207499), *cis*-4-cyano-4-(3-cyclopentyloxy-4-methoxyphenyl)-(*R*)-1-cyclohexanecarboxylic acid; SPA, scintillation proximity assay; UCR, upstream conserved region.

10.1021/bi010096p CCC: $20.00
Published on Web 08/01/2001

desirable inhibitory effects on inflammation and smooth muscle contraction, many of them produce undesirable side effects, including nausea and vomiting as typified by (*R*)-rolipram (*16*, *17*). Consequently, there has been a vigorous pursuit of inhibitors with an improved therapeutic index. However, structure-based inhibitor design had been limited by the lack of understanding of their PDE4 interaction at the molecular level. Earlier studies measuring the binding of inhibitors with PDE4 relied on a nonequilibrium filtration binding assay, which was limited by its incomplete capturing of the ligand/PDE4 complex and the rapid dissociation of low-affinity complexes during the washing process (*18*). The FRET-based equilibrium binding assay, which is capable of continuously monitoring the occupancy of the PDE4 active site in the presence and absence of Mg^{2+}, is sensitive to color interference above 285 nm, thereby limiting its utility (*7*). We have now overcome these limitations by developing an equilibrium-based [^{3}H]rolipram binding assay, utilizing the phenomenon of scintillation proximity. The assay relies on the fact that only β-particles from bound [^{3}H]rolipram are in close enough proximity to efficiently excite the scintillant inside the SPA beads (*s*cintillation *p*roximity *a*ssay, Amersham Pharmacia Biotech). Herein we report the characterization of the assay and its utility in dissecting the cofactor-dependent and independent binding of inhibitors and the PDE4 catalytic machinery.

EXPERIMENTAL PROCEDURES

Chemicals. SPA−PDE beads, SPA−protein A beads (yttrium−silicate and PVT based), [^{3}H]-(*R*)-rolipram (specific radioactivity 24 Ci/mmol, custom synthesized), [^{3}H]-(*R/S*)-rolipram (specific radioactivity 85 Ci/mmol), *d*-[8,9-^{3}H]biotin (specific activity 32 Ci/mmol), and [^{3}H]cAMP were purchased from Amersham International Inc. IBMX was purchased from Aldrich. Other PDE4 inhibitors were prepared at Merck Frosst. Rabbit anti-GST antibody was obtained from Molecular Probes. DEAE-Sepharose, Q-Sepharose, glutathione−Sepharose 4B, and the Mono-Q ion-exchange column were purchased from Pharmacia. Complete protease tablet was from Boehringer Mannheim. Other chemicals were from Sigma/Aldrich.

PDE4 Expression and Purification. PDE4A$^{248-886}$ of HSPDE4A4B was expressed as a GST fusion protein and purified to homogeneity on a Mono-Q column in the presence of 5 mM EDTA after eluting from a GST−Sepharose bead as previously described (*7*). The protein was stored at − 80 °C in a buffer containing 20% (v/v) glycerol, 1 mM EDTA, 1 mM DTT, 20 mM HEPES (pH 7.2), and 200 mM KCl. Protein concentration was determined on the basis of its absorbance at 280 nm using an extinction coefficient of 1.0 $mg^{-1}\cdot mL^{-1}\cdot cm^{-1}$. Under the conditions from the extended exposure to EDTA, PDE4A carries an insignificant amount of Zn^{2+} or other divalent cations from atomic absorption spectroscopy analysis (*6*).

PDE Activity Assay. Hydrolysis of [^{3}H]cAMP to [^{3}H]AMP by PDE4 was monitored using the PDE−SPA beads as previously described (*7*). The total ionic strength of solutions used in divalent cation titration was maintained at 150 mM with KCl. No specific ion effects were detected for either K^+ or Cl^- ions. Trace divalent cations were removed by treating buffers overnight with a K^+ form of Chelex beads (Bio-Rad) which were generated as follows: Chelex beads (20 mL bed volume), washed with 3 × 200 mL of 6 N HCl and 3 × 200 mL of H_2O, were incubated with 150 mL of 20 mM EDTA overnight to remove adventitious divalent cations. The resulting beads were washed with 3 × 200 mL of 500 mM KCl and 10 mM EDTA to exchange the H^+ to K^+ form. Excess KCl was washed away with a buffer containing 5 mM HEPES (pH 7.2), 1 mM EDTA, and 5 mM ultragrade KCl until the pH returned to neutral.

Active Site Titration. PMNPQ (5 nM) was incubated at room temperature for 10 min with increasing concentrations of GST−PDE4A^{248} in 150 μL buffer containing 20 mM HEPES (pH 7.2), 1 mM EDTA, 10 mM $MgCl_2$, and 100 mM KCl. After 15 min on ice, the reaction mixture was mixed with 15 μL of 20 μM [^{3}H]cAMP (10 μCi/mL) on ice to determine the remaining PDE activity for 60 s. The reaction was quenched instantly by the addition of 20 μL of 0.1 N HCl. Excess acid was neutralized with 30 μL of 1 M Tris (pH 7.5) before the quantification of [^{3}H]AMP. The interception point between the initial and the second linear phase of the residual PDE activity vs enzyme concentration plot was used to estimate the effective active site concentration.

Filtration-Based Rolipram Binding Assay. [^{3}H]-(*R*)-Rolipram binding to GST−PDE4A^{248} in a filtration assay was determined as previously described (*6*). GST−PDE4A^{248} (1 μg) was incubated for 10 min at room temperature in a 100 μL buffer containing 20 mM HEPES (pH 7.2), 1 mM EDTA, and 6 mM Mg^{2+}, with 0.1−100 nM [^{3}H]-*(R)*-rolipram, prior to rapid filtration (Tomtec Harvester-96) through GF/B filters presoaked in 1% polyethylenimine. The filters were washed with ice-cold buffer and counted.

SPA-Based Rolipram Binding Assay. Typically, GST−PDE4A^{248} was added to a 150 μL buffer, in a 96-well plate, containing 2 μg of anti-GST antibody, 100 mM KCl, 20 mM HEPES (pH 7.2), 6 mM Mg^{2+}, and 1 mM EDTA (for the holoenzyme) or 10 mM EDTA (for the apoenzyme). For inhibitor competition studies, 1.6 nM [^{3}H]-(*R*)-rolipram and 5 nM GST−PDE4A^{248} were used in the presence of 5 mM Mg^{2+}. A 20 nM quantity of the less expensive [^{3}H]-(*R/S*)-rolipram and 10 nM GST−PDE4A^{248} were used in the presence of 10 mM EDTA. Inhibitors were introduced via 2 μL DMSO solutions, which exerted a negligible effect at a final concentration of 1% (v/v). The mixture was incubated for 15 min at room temperature before the addition of 1 mg (∼50 pmol) of the protein A coated SPA beads in 50 μL of assay buffer. The bound radioactivity was counted on a Wallac Microbeta counter after being shaken for >20 min at room temperature. A stable count was established within 15 min after the addition of SPA beads. For K_d and B_{max} determination, [^{3}H]-(*R*)-rolipram was varied from 0.1 to 50 nM, and [^{3}H]-(*R/S*)-rolipram was varied from 0.1 to 500 nM. The reproducibility above 350 nM rolipram deteriorated rapidly due to an increasing nonspecific binding. Nonspecific binding was nearly identical among solutions lacking either enzyme or anti-GST antibody. The counting efficiency of the Microbeta counter was calibrated using a freshly prepared [^{3}H]biotin/PVT−SPA streptavidin complex assuming quantitative capture of biotin. The detection efficiency for [^{3}H]biotin in the SPA mode with PVT beads was at 11 (±2) CPM per 100 dpm of [^{3}H]biotin. The metal ion requirement for [^{3}H]-(*R*)-rolipram binding to PDE4 was determined while

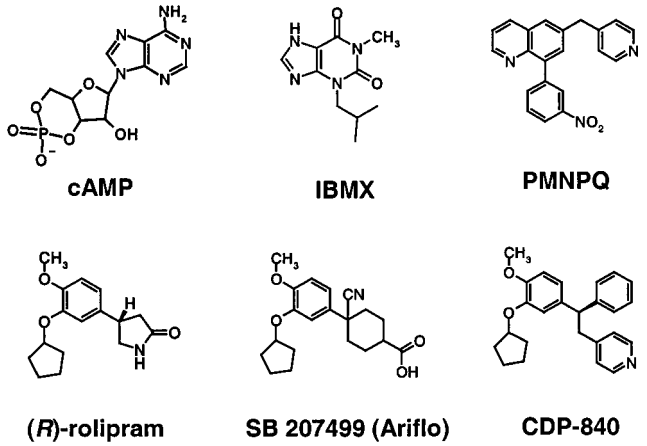

FIGURE 1: Structures of cAMP and inhibitors.

the total ionic strength was maintained at 150 mM with KCl. No specific ion effects were observed for either K^+ or Cl^- ions. Trace divalent cations were removed from buffers with the K^+ form of the Chelex beads as described above. Anti-GST antibody was exchanged into the metal-free buffer using a Centricon-30 (Millipore). SPA−protein A beads were washed with a buffer containing 1 mM EDTA, 20 mM HEPES (pH 7.2), and 130 mM KCl before being suspended in the metal-free buffer. Both polyvinyltoluene (PVT)-based protein A scintillation beads (more amenable to automation due to its reduced density difference with water) and yttrium−silica-based protein A scintillation beads were used with comparable results obtained for most inhibitors. IC_{50} values for some hydrophobic inhibitors such as CDP-840 were increased using the PVT beads, which was traced to their absorption by the matrix.

Data Analysis. Data are expressed as mean ± SE of n ($\geq$3) independent experiments unless otherwise specified. Dose responses were analyzed using the Grafit curve-fitting program (Erithacus Software). IC_{50} values were determined from the analysis of 11-point dose−response curves performed in duplicate.

RESULTS

High- and Low-Affinity Rolipram Binding to PDE4 in the Presence and Absence of Mg^{2+}. Recombinant PDE4A^{248}, lacking the N-terminal amino acids 1−247 of HSPDE4A4B and representing the common region of the multiple PDE4A splice variants, was expressed in a baculovirus/Sf9 expression system as a GST fusion protein and purified to greater than 95% homogeneity. Earlier studies, comparing PDE4A$^{1-886}$ and PDE4A^{248} expressed in COS cells, indicated that both enzymes bound (*R*)-rolipram with a similar high affinity (K_d $\sim$ 3 nM) in a filtration assay and possessed comparable activities in hydrolyzing cAMP (*19*). In the presence of 5 mM Mg^{2+} in the same filtration assay, (*R*)-rolipram bound specifically to GST−PDE4A^{248} with a K_d value of $\sim$3 nM and a low binding stoichiometry, which varied between 0.01 and 0.001 mole fraction (mole of rolipram per mole of PDE4) depending on the washing duration (data not shown). This low and variable binding stoichiometry signifies an incomplete capture of the enzyme/rolipram complex. The results are comparable with that of PDE4A$^{201-886}$ and PDE4A$^{256-886}$ (*20*). In the absence of Mg^{2+}, a very low specific binding ($\sim$10% of the background) was detected at 100 nM [^{3}H]-(*R*)-rolipram in the filtration assay, and the signal was too scattered to work with. This binding was reduced by the presence of 200 nM PMNPQ [6-(4-pyridylmethyl)-8-(3-nitrophenyl)quinoline] (Figure 1), a potent PDE4 inhibitor (*21*) with an IC_{50} value of 0.07 nM at inhibiting GST−PDE4A^{248} catalysis.

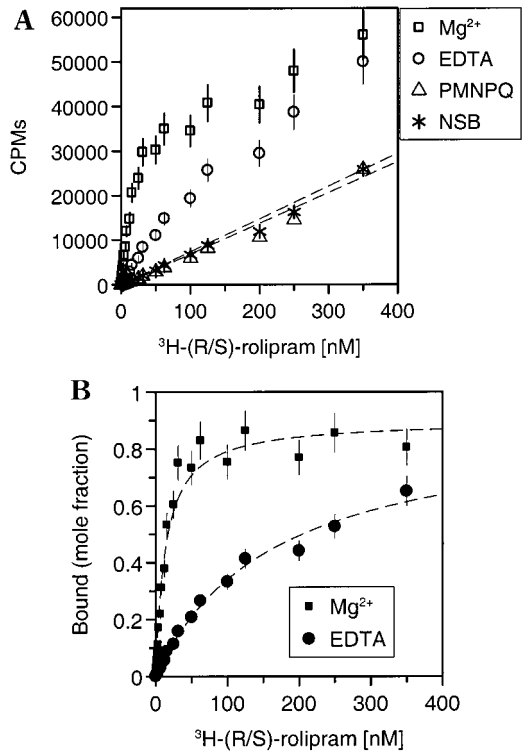

FIGURE 2: Mg^{2+}-dependent and Mg^{2+}-independent binding of [^{3}H]-(*R/S*)-rolipram to GST−PDE4A^{248} in the SPA-based binding assay. (A) Radioactivity (cpm) bound to the SPA beads from solutions containing (□) GST−PDE4A^{248} (0.2 μg) + 6 mM Mg^{2+} + 1 mM EDTA; (○) GST−PDE4A^{248} (0.2 μg) + 10 mM EDTA; (△) GST−PDE4A^{248} (0.2 μg) + 10 mM EDTA + PMNPQ (200 nM) (the values were similar in the presence of Mg^{2+}); (*) GST−PDE4A^{248} (0 μg) (the values were similar to samples missing anti-GST antibody and they were insensitive to Mg^{2+}). The dashed lines are the linear fits for (*) and (△). (B) The specifically bound radioactivity [mole fraction: mole of (*R/S*)-rolipram per mole of PDE4] with respect to increasing [^{3}H]-(*R/S*)-rolipram in the presence (■) and absence (●) of Mg^{2+} from panel A after subtracting the nonspecific signals. Saturation analysis with the single binding site model (dashed lines) gave a K_d value of 13 (±2) nM with a B_{max} value of 0.83 (±0.07) mole fraction in the presence of Mg^{2+} and an estimated racemic K_d value of 170 (±30) nM with a B_{max} value of 0.9 (±0.1) mole fraction in the absence of Mg^{2+}. The data represent the mean of three experiments.

To overcome the limitations of the filtration assay, an equilibrium-based [^{3}H]rolipram binding assay was developed, which used the SPA−protein A/anti-GST/GST−PDE4 format. Thus, GST−PDE4A^{248} was immobilized to the SPA−protein A beads via an anti-GST antibody. Shown in Figure 2A are the radioactivity counts bound to the immobilized enzyme with respect to increasing [^{3}H]-(*R/S*)-rolipram concentration in the presence of 5 mM Mg^{2+} (□) and 10 mM EDTA (○). The latter ensures the removal of adventitious divalent cations. The nonspecific binding (NSB) in the absence of PDE4 (*) increased linearly with increasing [^{3}H]-(*R/S*)-rolipram concentration and was insensitive to the presence of Mg^{2+} or inhibitors. The nonspecific binding was also comparable with solutions lacking anti-GST antibody.

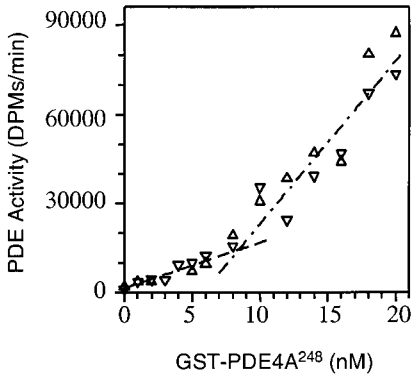

FIGURE 3: Active site titration using PMNPQ. Increasing concentrations of GST−PDE4A^{248} (based on its absorbance at A_{280}) were incubated with 5 nM PMNPQ for 10 min at room temperature. The residual PDE activity (in duplicates) was measured for 60 s on ice. The initial linear phase intercepted with the second linear phase near 7 (±1) nM GST−PDE4A^{248}. The slope of the second linear phase was identical to that observed in the absence of PMNPQ (data not shown).

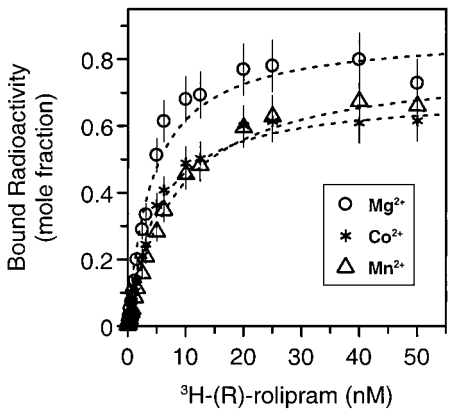

FIGURE 4: [^{3}H]-(*R*)-Rolipram binding to GST−PDE4A^{248} in the presence of 5 mM Mg^{2+}(○), 5 mM Mn^{2+} (△), and 5 mM Co^{2+} (*). Nonlinear regression analysis gave a K_d of 3.5 (±0.6) nM and a B_{max} of 0.81 (±0.08) mole fraction for Mg^{2+}, a K_d of 4.7 (±1) nM and a B_{max} of 0.65 (±0.07) mole fraction for Co^{2+}, and a K_d of 8 (±1) nM and a B_{max} of 0.73 (±0.07) mole fraction for Mn^{2+}. The data represent the mean of three experiments.

PMNPQ (200 nM) completely abolished the PDE4-mediated [^{3}H]-(*R/S*)-rolipram binding in the presence and absence of Mg^{2+}, with the residual radioactivity (△) superimposable on the NSB (*). The results indicate that PDE4-mediated [^{3}H]-(*R/S*)-rolipram binding is specific in the presence and absence of Mg^{2+}. Shown in Figure 2B is the corresponding specific rolipram binding to PDE4 after subtraction of the nonspecific (*) responses. In the presence of Mg^{2+} (■), the saturation binding had an apparent K_d of 13 nM with a B_{max} of 0.83 mole fraction for the racemic (*R/S*)-rolipram. In the absence of Mg^{2+}, the specific binding (●) increased with increasing concentration of [^{3}H]-(*R/S*)-rolipram. The linearly increasing nonspecific signal overtook the magnitude of the specific signal above 350 nM, leading to increased data scattering. This limited us in obtaining a full saturation response under the conditions. Analysis of the specific binding in the absence of Mg^{2+}, using a single binding site model, gave a K_d value of 170 nM for racemic (*R/S*)-rolipram and a projected B_{max} of 0.9 mole fraction.

The specific [^{3}H]rolipram binding to PDE4 in the presence and absence of Mg^{2+} is reversible judging from its rapid displacement by unlabeled rolipram at room temperature. Over 90% of the PDE4-bound [^{3}H]rolipram was displaced by 5 μM (*R*)-rolipram within 2 min, the first point measurable on the Microbeta counter. In the presence of 10 μg/mL anti-GST antibody, the specific binding in the presence or absence of Mg^{2+} was linear with respect to increasing GST−PDE4A^{248} concentration up to 2 μg/mL (~20 nM). Further increases in anti-GST antibody concentration under these conditions exerted a negligible effect on the specific binding in the presence and absence of Mg^{2+}, supporting the complete capture of enzyme under the conditions used. In the presence of 5 mM Mg^{2+} and 1.6 nM [^{3}H]-(*R*)-rolipram, the specific to nonspecific binding ratio exceeded 10 to 1 with the use of ≥0.3 μg/mL (3 nM) GST−PDE4A^{248}. In the absence of Mg^{2+}, 10 nM of GST−PDE4A^{248} was required to maintain a corresponding ratio of ≥2:1 at 20 nM of [^{3}H]-(*R/S*)-rolipram. These protein concentrations set the lower limits of the assay for determining dissociation constants.

To measure the active site concentration of PDE4, the residual PDE activity of increasing concentrations of GST−PDE4A^{248} after incubation with 5 nM PMNPQ was determined by the addition of [^{3}H]cAMP (1 μM) for 60 s at 0 °C. This procedure limited the dissociation of the PMNPQ/PDE4 complex with the residual activity directly proportional to the free enzyme. A biphasic, linear dose−response curve with an intercept at ~7.5 nM enzyme was obtained (Figure 3), with the slope of the second linear phase paralleling that in the absence of PMNPQ (data not shown). The result indicates that ~70% of the protein was active, assuming a stoichiometric PMNPQ binding to PDE4. The active site concentrations of several batches of GST−PDE4A^{248} ranged from 0.6 to 0.9 mole fraction. After correction for the presence of inactive protein, the 0.8−0.9 mole fraction of [^{3}H]rolipram binding to PDE4 measured in the presence and absence of Mg^{2+} became essentially stoichiometric.

Table 1: Comparison between the Metal Cation Requirements for Catalysis and [^{3}H]-(*R*)-Rolipram Binding to GST−PDE4A^{248}

	EC_{50} (μM)[a]			
cofactor	catalysis	rolipram binding	K_d (nM) (*R*)-rolipram	rolipram binding stoichiometry (mole fraction)
Mg^{2+}	100 ± 11	125 ± 45	3.5 ± 0.6	0.81 ± 0.08
Co^{2+}	6 ± 1	8 ± 2	4.7 ± 1	0.65 ± 0.07
Mn^{2+}	3 ± 1	7 ± 3	8 ± 1	0.73 ± 0.07

[a] EC_{50} values (mean ± SE, $n = 4$) for catalysis were determined using 0.1 μM cAMP. EC_{50} values (mean ± SE, $n = 3$) for rolipram binding were determined using 1.6 nM [^{3}H]-(*R*)-rolipram. The K_d values of (*R*)-rolipram were determined in the presence of a saturating concentration (5 mM) of Mg^{2+}, Mn^{2+}, or Co^{2+}. The stoichiometry of (*R*)-rolipram binding was calculated without correcting for the active site concentration of PDE4.

Divalent Cation Mediated High-Affinity (R)-Rolipram Binding to PDE4. Figure 4 shows the dose responses obtained for the binding of the (*R*)-enantiomer of [^{3}H]rolipram to GST−PDE4A^{248} in the presence of saturating concentrations (5 mM) of Mg^{2+} (○), Mn^{2+} (△), and Co^{2+} (*). A K_d value of 3.5 nM with a unit Hill coefficient (0.97 ± 0.08) was obtained in the presence of Mg^{2+} for the (*R*)-enantiomer with a binding stoichiometry close to 1 (0.8 mole fraction without correcting for the active site concentration). Similar high affinities, with near stoichiometric rolipram binding to PDE4, were observed in the presence of Mn^{2+} and Co^{2+} (summarized in Table 1).

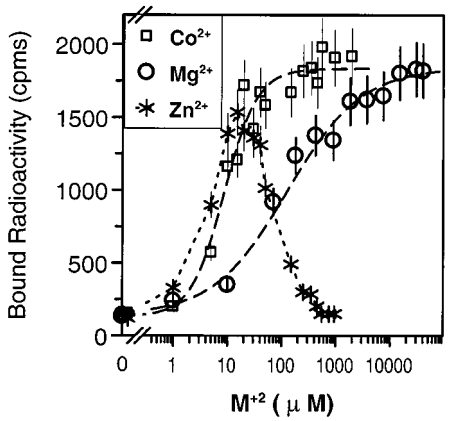

FIGURE 5: Dose responses of Mg^{2+} (○), Co^{2+} (□), and Zn^{2+} (*) mediated [^{3}H]-(*R*)-rolipram (1.6 nM) binding to GST−PDE4A^{248} in the SPA-based binding assay. The metal ion concentrations at the half-maximal responses were at 125 (±45) μM for Mg^{2+}, 8 (±2) μM for Co^{2+}, and 1−5 μM for Zn^{2+}. The data represent the mean of three experiments.

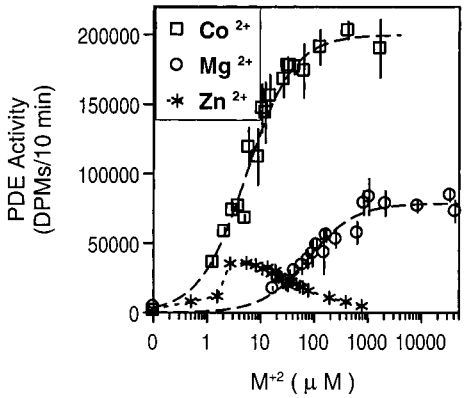

FIGURE 6: Dose responses of Mg^{2+} (○), Co^{2+} (□), and Zn^{2+} (*) mediated hydrolysis of [^{3}H]cAMP by GST−PDE4A^{248} in the presence of 0.1 μM [^{3}H]cAMP. The EC_{50} values were at 100 (±11) μM for Mg^{2+} and 6 (±1) μM for Co^{2+}, respectively. The maximal activity in the presence of Co^{2+} was ~2.5 times that of Mg^{2+}. Similar maximal activities were observed using a saturating concentration of cAMP (10 μM).

Figure 5 shows the effectiveness of Co^{2+} (□), Mg^{2+}, (○), and Zn^{2+} (*) in stimulating [^{3}H]-(*R*)-rolipram binding to GST−PDE4A^{248}. The response curve for Mn^{2+}, which superimposed on that of Co^{2+}, is not displayed for clarity. The saturation curves had EC_{50} values of 125 μM for Mg^{2+}, 7 μM for Mn^{2+} and 8 μM for Co^{2+}. Zn^{2+}-dependent specific (*R*)-rolipram binding to PDE4 peaked between 2 and 8 μM and decreased rapidly after 50 μM, with the maximal response approaching those of Mg^{2+}, Mn^{2+}, and Co^{2+}. Shown in Figure 6 are the corresponding dose−response curves for these divalent cations in activating the GST−PDE4A^{248}-catalyzed hydrolysis of 0.1 μM [^{3}H]cAMP. In the absence of cofactor ions, no cAMP turnover was detected. The EC_{50} values are 100 μM for Mg^{2+} (○), 6 μM for Co^{2+} (□), and 3 μM for Mn^{2+} (which paralleled that of the Co^{2+} response and is not displayed for clarity). Activation by Zn^{2+} (*) exhibited a biphasic dose−response curve, similar to that observed with the [^{3}H]rolipram binding, peaked between 2 and 5 μM and decreased after 50 μM. Protein aggregation at higher Zn^{2+} concentrations has been suggested to be responsible for a similar Zn^{2+}-mediated activity inhibition of PDE6 (*22*). The results indicate that the divalent cation requirements for inducing the high-affinity (*R*)-rolipram binding to PDE4 mirror their corresponding efficacy in catalysis.

Table 2: Potency of cAMP and AMP in Displacing the Apo- and Holoenzyme-Bound Rolipram[a]

compound	IC_{50} (μM) holoenzyme	IC_{50} (μM) apoenzyme
cAMP	(K_s = 1.9)[b]	179 ± 54
AMP	7300 ± 350	11000 ± 2900

[a] IC_{50} values (mean ± SE, n = 3) were determined using 3 nM GST−PDE4A^{248}, 1.6 nM [^{3}H]-(*R*)-rolipram, and 5 mM Mg^{2+} for the holoenzyme and 10 nM GST−PDE4A^{248}, 20 nM [^{3}H]-(*R/S*)-rolipram, and 10 mM EDTA for the apoenzyme. Under the conditions, the IC_{50} values were close to their K_d. [b] The rapid cAMP turnover in the presence of Mg^{2+} prevented the accurate measurement of its holoenzyme binding affinity in the SPA binding assay. Its K_s value was from ref *7*.

Displacement by cAMP and AMP. Similar to earlier reports (*19*, *20*, *23*), cAMP efficiently competed with (*R*)-rolipram binding to PDE4 in the SPA binding assay. At room temperature, >80% of the holoenzyme- bound [^{3}H]-(*R*)-rolipram was displaced by an initial dose of 50 μM cAMP within 2 min. The displacement occurred despite the rapid hydrolysis of cAMP, which prevented the estimation of its affinity under the conditions. This is consistent with the K_s value of 1.9 μM for cAMP binding to the holoenzyme detected in the FRET binding assay (*7*). In the absence of metal cations, cAMP displaced the apoenzyme-bound [^{3}H]rolipram with an IC_{50} value of 179 μM and a near unit Hill coefficient (Table 2). Thus rolipram binding is mutually exclusive with cAMP to both PDE4 apo- and holoenzyme. AMP displaced the bound rolipram from the holo- and apoenzyme with IC_{50} values of 7.3 and 11 mM, respectively. The high absorbance of AMP near 285 nm above 1 mM prevented it being studied in the FRET binding assay (*7*).

Competition by Inhibitors. The specific and reversible binding of [^{3}H]rolipram to both holo- and apoenzyme, coupled with the mix/read feature of the SPA-based binding assay, enabled the rapid delineation of the affinities of inhibitors with the two conformers. (*R*)- and (*S*)-rolipram competed differentially with the binding of [^{3}H]-(*R*)-rolipram to the holoenzyme with IC_{50} values of 5 nM (●) and 64 nM (▲) (Figure 7). The 12-fold stereoselectivity toward the holoenzyme was reduced to ~2-fold toward the apoenzyme with IC_{50} values of 150 nM (○) for (*R*)- and 290 nM (△) for (*S*)-rolipram. The potencies of the individual enantiomers compare well with the apparent K_d of ~170 nM for the racemic (*R/S*)-rolipram with the apoenzyme from Figure 2B. The small difference in affinities between the (*R*)- and (*S*)-enantiomers against the apoenzyme allowed the use of less expensive racemic [^{3}H]-(*R/S*)-rolipram in competition studies without introducing noticeable biphasic behavior. Table 3 lists the IC_{50} values of a representative set of PDE4 inhibitors in displacing bound rolipram from the holo- and apoenzyme. A structure-dependent differential competition was observed. IBMX, a xanthine-based inhibitor with a catalytic potency (IC_{50}) of 4 μM against PDE4, showed little difference in displacing bound rolipram between the apo- and holoenzyme. Its strong absorption near 285 nm, like many other inhibitors with extended conjugation, precluded it from being evaluated in the FRET binding assay. In contrast, CDP-840 and Ariflo competed exclusively with the holoenzyme binding of (*R*)-

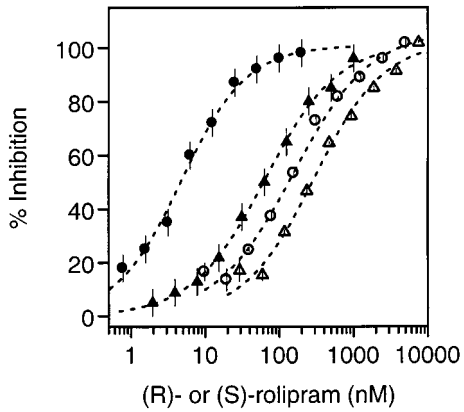

FIGURE 7: Displacement of [^{3}H]-(*R*)-rolipram (1.6 nM) binding to the PDE4 holoenzyme by (*R*)- (●) and (*S*)-rolipram (▲) and the displacement of [^{3}H]-(*R/S*)- rolipram binding to the apoenzyme by (*R*)- (○) and (*S*)-rolipram (△). Where they do not appear, the errors are within the symbols. The IC_{50} values for (*R*)- and (*S*)-rolipram were at 5 (±1) nM and 64 (±4) nM with the holoenzyme and 150 (±37) nM and 290 (±68) nM with the apoenzyme, respectively. The data represent the mean of three experiments.

Table 3: Apoenzyme and Holoenzyme Affinities of PDE4 Inhibitors and Their Catalytic Potency[a]

	IC_{50} (nM)		
compound	holoenzyme	apoenzyme	catalytic potency
(*R*)-rolipram	5 ± 1	150 ± 37	5 ± 3
(*S*)-rolipram	64 ± 4	290 ± 68	70 ± 15
Ariflo	42 ± 7	>4000	37 ± 15
CDP-840	20 ± 5 6 ± 2 (silica)	>4000	3 ± 1
IBMX	2200 ± 500	4700 ± 400	4000 ± 1000
PMNPQ	≤3[b]	≤10[b]	0.07 ± 0.05

[a] IC_{50} values (mean ± SE, $n \geq 3$) were determined using 3 nM GST−PDE4A^{248}, 1.6 nM [^{3}H]-(*R*)-rolipram, and 5 mM Mg^{2+} for the holoenzyme and 10 nM GST−PDE4A^{248}, 20 nM [^{3}H]-(*R/S*)-rolipram, and 10 mM EDTA for the apoenzyme. Similar values were obtained using PVT-based or yttrium−silicate-based SPA beads except for CDP-840, which was partially absorbed by the PVT matrix. The catalytic potencies were determined using 0.1 μM cAMP and 10 mM Mg^{2+}. [b] Detection limit.

rolipram. The apparent IC_{50} values of 3 nM (holoenzyme) and 10 nM (apoenzyme) for PMNPQ were both at the detection limits of the assay. These binding affinities are comparable with those obtained in the FRET binding assay, suggesting that the immobilization of PDE4 exerts a negligible effect on its active site conformation. Table 3 also lists the catalytic potency (IC_{50}) of these inhibitors under a saturating concentration of Mg^{2+} (10 mM). They compared well with their holoenzyme affinities.

DISCUSSION

Since the initial report of the Mg^{2+}-stimulated high affinity (K_d ~2 nM) and stereoselective binding of (*R*)-rolipram in rat brain homogenates (*18*), its potent pharmacological activities and multiphasic interactions with PDE4 have attracted considerable attention (*20, 24*−*27*). Detailed mutational, calorimetric, and binding studies have identified the presence of two coexisting rolipram/PDE4 interactions within the active site (*28*−*31*). We have recently clarified that the reversible Mg^{2+} binding to PDE4 is responsible for eliciting the differential rolipram interaction (*7*). In the present study, we have further quantified the rolipram/PDE4 interactions and identified that Mg^{2+}, Mn^{2+}, and Co^{2+} all mediate a similar high affinity (K_d 3−8 nM) and stoichiometric rolipram binding to PDE4. In their absence, a low-affinity and stoichiometric rolipram binding to the apoenzyme is detected.

Of the two cofactor ions in the binuclear center, M_1 is bound more tightly as illustrated in Figure 8 (*11*). The binding of both cofactor ions in PDE4 remains reversible as evidenced by the lack of significant amount of divalent cations in PDE4A purified in the presence of EDTA (*6*). The PDE4A apoenzyme binds Zn^{2+} stoichiometrically and reversibly with a K_d of ~0.4 μM in the absence of cAMP, and the bound Zn^{2+} was only partially displaced by 50 mM Mg^{2+} (*6*), supporting its M_1 position. The PDE4-bound Zn^{2+} behaved closely to that in PDE5 (*32*). In comparison, a stronger Zn^{2+} binding (low nanomolar K_d) was detected in the cGMP-specific PDE6, an enzyme with a near perfected catalytic machinery (k_{cat} ~7000 s^{-1}) (*22*). Approximately 70% of the PDE6 activity was lost after an overnight EDTA treatment, implying that its tightly bound Zn^{2+} was also removed upon the extended EDTA exposure (*22*). It is unclear whether the difference in cofactor binding affinities between PDE4 and PDE6 contributes to their k_{cat} difference (~17 s^{-1} in PDE4) (*7*). The presence of 10 mM EDTA, coupled with the use of enzyme purified in the presence of EDTA, ensures a divalent cation-free environment for the apoenzyme in the present study. Thus, the monophasic dose responses of Mg^{2+}, Mn^{2+}, and Co^{2+} in activating the PDE4 activity are most simply explained by the hypothesis that they are indexing the binding of M_2 after M_1 is already in position in the binuclear ion center. Their similar dose responses in stimulating the high-affinity (*R*)-rolipram binding to PDE4 support the notion that both cations of the holoenzyme are involved in the high-affinity rolipram/PDE4 interaction with the dose response reflecting the binding of M_2. The absence of a biphasic dose response may imply the possible presence of synergism or the dose−response range from M_1 binding alone is very narrow. Efforts are underway in an attempt to characterize the corresponding cofactor complexes.

The 94-fold enhanced binding of cAMP to the holoenzyme (K_s ~1.9 μM) over the apoenzyme (K_d ~179 μM), initially detected in the FRET binding assay (*7*), is confirmed here using the immobilized enzyme. After accounting for the 24 mM (K_d) binding between cAMP and Mg^{2+} in solution (*33*), the data support a direct phosphate/Mg^{2+} interaction in the cAMP/holoenzyme complex, consistent with the docked position of cAMP in PDE4B (Figure 8) (*11*). Hydrogen-bonding and hydrophobic interactions between the adenosine moiety and its proximal residues could contribute to the 179 μM cAMP/apoenzyme interaction. The Mg^{2+}-mediated cAMP/holoenzyme interaction becomes negligible in the corresponding AMP/holoenzyme complex (7.3 mM with the holoenzyme vs 11 mM with the apoenzyme), suggesting that the hydrolysis and opening of the cyclic phosphoester bond of cAMP disrupts most of the Mg^{2+}/phosphate interaction in the cAMP/holoenzyme complex. Together with the ~60-fold reduced AMP binding to the apoenzyme in comparison to that of cAMP, this contributes to the lack of a significant product inhibition in PDE4 catalysis. On the other hand, the remaining weak AMP/holoenzyme binding (7.3 mM) could be contributing to the decreased cAMP turnover in PDE4 in

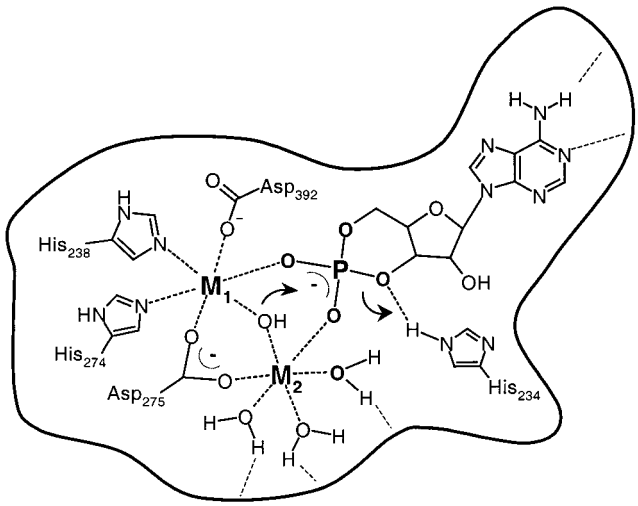

FIGURE 8: Mechanistic roles of the binuclear ion center for cAMP binding and catalysis in PDE4. The two divalent cations are labeled as M_1 and M_2. Amino acids proximal to the ion center are numbered according to their positions in PDE4B2B (*11*). In the model, both metal ions coordinate to the phosphoryl oxygens to elicit a high-affinity cAMP binding and to increase the phosphate electrophilicity. Either the bridging hydroxide or a M_2-coordinated water acts as the nucleophile, and catalysis is further assisted by a hydrogen-bonding interaction between the conserved His^{234} and the O3′ leaving group (*11*, *39*). The cofactor-dependent cAMP binding to PDE4 diminishes upon the hydrolysis of the cyclic phosphoester bond.

comparison with that in PDE6 (*22*). Coupled with molecular simulation, these data could help to build a reaction trajectory for cAMP hydrolysis and AMP release in PDE4.

In the past, the potency of an inhibitor in activity inhibition was thought to reflect its binding to a "*low-affinity PDE4 conformer*". We have named this kinetic parameter as the *catalytic potency* of an inhibitor, which differs from its binding affinity with the apoenzyme (*7*). Although only the holoenzyme is catalytically active, inhibitor binding to the other coexisting conformer also leads to inhibition of catalysis. This causes the catalytic potency to partition between its apoenzyme and holoenzyme binding affinities (*7*, *34*). For inhibitor that binds exclusively to the holoenzyme, the catalytic potency directly indexes its holoenzyme binding affinity, which can also be detected by monitoring the displacement of the rolipram/holoenzyme interaction. On the other hand, the catalytic potency of a dual binding inhibitor is dictated by (a) the Mg^{2+} concentration, (b) the Mg^{2+} binding affinity of the enzyme, and (c) the rate-limiting transition between the coexisting conformers in comparison with cAMP turnover. Under the rapid equilibrium assumption with cAMP hydrolysis being rate limiting, the catalytic potency of a dual binding inhibitor partitions favorably toward its holoenzyme binding affinity under a saturating Mg^{2+} concentration (*34*). Complications arise from either a heterogeneous PDE4/Mg^{2+} interaction or the rate-limiting transition being shifted away from cAMP hydrolysis. For example, a rapid inhibitor/apoenzyme complex, coupled with a rate-limiting formation of its holoenzyme complex, would lead to the catalytic potency to partition favorably toward its apoenzyme binding affinity even under a saturating Mg^{2+} concentration. This may be related to the time-dependent formation of the high-affinity rolipram/PDE4B complex reported (*29*, *31*).

The N-terminal domains of PDE4s and their interaction with proteins or membranes exert profound effects on cAMP hydrolysis (*8*, *26*, *35*−*37*). Their causes could be multifactorial and remain to be dissected individually. The binuclear center of PDE4 is located at the interface of three subdomains (*11*). It is tempting to speculate that the cofactor binding affinity may be sensitive to some perturbations within these domains. It is intriguing to note that some of these interactions selectively modulate the catalytic potency of rolipram without significantly altering the potencies of inhibitors that are now known to interact selectively with the holoenzyme (*8*, *20*, *26*), implying that they exert minimal perturbations on the holoenzyme/inhibitor interaction. This phenomenon could be explained using the current model if one proposes that these interactions are mainly affecting the cofactor binding or modulating the transitions among the interconverting conformers. The increased Mg^{2+} binding through Ser^{54} phosphorylation in PDE4D3 (*8*) and the variable Mg^{2+} affinities among PDE4A deletion mutants (*38*) appear to support the speculation. Further studies including the identification of the rate-limiting transition can help to clarify the remaining issues of PDE4 inhibition.

The PDE4 active site is formed by amino acids residing on several α-helices (*11*). Its limited flexibility favors the hypothesis that the conformational difference between the apo- and holoenzyme is localized near the binuclear ion center with the other area remaining conserved. The lack of a detectable change in the protein intrinsic fluorescence upon Mg^{2+} binding (*7*) and the dual binding of cAMP, AMP, and diverse inhibitors such as rolipram, IBMX, and PMNPQ are all in favor of the hypothesis. In contrast to cAMP, the nature of the metal ion-dependent binding of inhibitors to PDE4 remains elusive. Either a direct chelation with the binuclear center or an interaction with residues perturbed by the presence of the ions could give rise to a metal ion-dependent inhibitor binding to PDE4. An altered topology around the binuclear center could also preclude the binding of some inhibitors in the absence of the metal ions. On the other hand, inhibitors residing away from the binuclear center could bind to both conformers regardless of its occupancy state. The last scenario may be relevant to the metal ion-insensitive binding of IBMX; its structure resembles the adenine portion of cAMP. Divergence among the active sites of the 11 families of PDEs occurs mainly away from the binuclear center (*11*). Thus, the metal ion-dependent and independent components of inhibitor binding to the active site provide the opportunity of using ion-chelating motifs within inhibitors to maximize their binding and to fine-tune the complementarity away from the binuclear center for selectivity.

In summary, the equilibrium [^{3}H]rolipram binding assay provides a robust tool to delineate the metal ion-dependent and independent binding of PDE4 inhibitors in a mix/read format. Coupled with molecular modeling, it provides the opportunity to design more potent and selective inhibitors using a modular approach.

ACKNOWLEDGMENT

The authors thank Ernest Asante-Appiah, Dave Percival, Brian Kennedy, and Ellie James for helpful discussions and critical reading of the manuscript.

REFERENCES

1. Fawcett, L., Baxendale, R., Stacey, P., McGrouther, C., Harrow, I., Soderling, S., Hetman, J., Beavo, J. A., and Phillips, S. C. (2000) *Proc. Natl. Acad. Sci. U.S.A. 97*, 3702−3707.
2. Conti, M., and Jin, S. L. (1999) *Prog. Nucleic Acid Res. Mol. Biol. 63*, 1−38.
3. Houslay, M. D., and Milligan, G. (1997) *Trends Biochem. Sci. 22*, 217−224.
4. Jin, S. L., Richard, F. J., Kuo, W. P., D'Ercole, A. J., and Conti, M. (1999) *Proc. Natl. Acad. Sci. U.S.A. 96*, 11998−12003.
5. Hansen, G., Jin, S., Umetsu, D. T., and Conti, M. (2000) *Proc. Natl. Acad. Sci. U.S.A. 97*, 6751−6756.
6. Percival, M. D., Yeh, B., and Falgueyret, J. P. (1997) *Biochem. Biophys. Res. Commun. 241*, 175−180.
7. Laliberte, F., Han, Y., Govindarajan, A., Giroux, A., Liu, S., Bobechko, B., Lario, P., Bartlett, A., Gorseth, E., Gresser, M., and Huang, Z. (2000) *Biochemistry 39*, 6449−6458.
8. Sette, C., and Conti, M. (1996) *J. Biol. Chem. 271*, 16526−16534.
9. Kovala, T., Sanwal, B. D., and Ball, E. H. (1997) *Biochemistry 36*, 2968−2976.
10. Donnelly, T. E. (1978) *Biochim. Biophys. Acta 522*, 151−160.
11. Xu, R. X., Hassell, A. M., Vanderwall, D., Lambert, M. H., Holmes, W. D., Luther, M. A., Rocque, W. J., Milburn, M. V., Zhao, Y., Ke, H., and Nolte, R. T. (2000) *Science 288*, 1822−1825.
12. Beese, L. S., and Steitz, T. A. (1991) *EMBO J. 10*, 25−33.
13. Torphy, T. J. (1998) *Am. J. Respir. Crit. Care Med. 157*, 351−370.
14. Torphy, T. J., Barnette, M. S., Underwood, D. C., Griswold, D. E., Christensen, S. B., Murdoch, R. D., Nieman, R. B., and Compton, C. H. (1999) *Pulm. Pharmacol. Ther. 12*, 131−135.
15. Giembycz, M. A. (2000) *Drugs 59*, 193-212.
16. Horowski, R., Sastre-y-hernandez, M. (1985) *Curr. Ther. Res. 38*, 23.
17. Barnette, M. S., Grous, M., Cieslinski, L. B., Burman, M., Christensen, S. B., and Torphy, T. J. (1995) *J. Pharmacol. Exp. Ther. 273*, 1396−1402.
18. Schneider, H. H., Schmiechen, R., Brezinski, M., and Seidler, J. (1986) *Eur. J. Pharmacol. 127*, 105−115.
19. Owens, R. J., Catterall, C., Batty, D., Jappy, J., Russell, A., Smith, B., O'Connell, J., and Perry, M. J. (1997) *Biochem. J. 326*, 53−60.
20. Jacobitz, S., McLaughlin, M. M., Livi, G. P., Burman, M., and Torphy, T. J. (1996) *Mol. Pharmacol. 50*, 891−899.
21. Wilhelm, R., Fatheree, P., and Chin, R. (1994) WO 94,22852.
22. He, F., Seryshev, A. B., Cowan, C. W., and Wensel, T. G. (2000) *J. Biol. Chem. 275*, 20572−20577.
23. Perry, M. J., O'Connell, J., Walker, C., Crabbe, T., Baldock, D., Russell, A., Lumb, S., Huang, Z., Howat, D., Allen, R., Merriman, M., Walls, J., Daniel, T., Hughes, B., Laliberte, F., Higgs, G. A., and Owens, R. J. (1998) *Cell Biochem. Biophys. 29*, 113−132.
24. Souness, J. E., and Rao, S. (1997) *Cell Signal. 9*, 227−236.
25. Jacobitz, S., Ryan, M. D., McLaughlin, M. M., Livi, G. P., DeWolf, W. E., Jr., and Torphy, T. J. (1997) *Mol. Pharmacol. 51*, 999−1006.
26. McPhee, I., Yarwood, S. J., Scotland, G., Huston, E., Beard, M. B., Ross, A. H., Houslay, E. S., and Houslay, M. D. (1999) *J. Biol. Chem. 274*, 11796−11810.
27. Huston, E., Pooley, L., Julien, P., Scotland, G., McPhee, I., Sullivan, M., Bolger, G., and Houslay, M. D. (1996) *J. Biol. Chem. 271*, 31334−31344.
28. Atienza, J. M., Susanto, D., Huang, C., McCarty, A. S., and Colicelli, J. (1999) *J. Biol. Chem. 274*, 4839−4847.
29. Rocque, W. J., Tian, G., Wiseman, J. S., Holmes, W. D., Zajac-Thompson, I., Willard, D. H., Patel, I. R., Wisely, G. B., Clay, W. C., Kadwell, S. H., Hoffman, C. R., and Luther, M. A. (1997) *Biochemistry 36*, 14250−14261.
30. Rocque, W. J., Holmes, W. D., Patel, I. R., Dougherty, R. W., Ittoop, O., Overton, L., Hoffman, C. R., Wisely, G. B., Willard, D. H., and Luther, M. A. (1997) *Protein Expression Purif. 9*, 191−202.
31. Tian, G., Rocque, W. J., Wiseman, J. S., Thompson, I. Z., Holmes, W. D., Domanico, P. L., Stafford, J. A., Feldman, P. L., and Luther, M. A. (1998) *Biochemistry 37*, 6894−6904.
32. Francis, S. H., Colbran, J. L., McAllister-Lucas, L. M., and Corbin, J. D. (1994) *J. Biol. Chem. 269*, 22477−22480.
33. Kobos, R. K., and Rechinitz, G. A. A. (1997) *Bioelectrochem. Bioenerg. 4*, 87−97.
34. Segel, I. H. (1993) *Enzyme Kinetics*, pp 273−329, John Wiley & Sons, New York.
35. Hoffmann, R., Wilkinson, I. R., McCallum, J. F., Engels, P., and Houslay, M. D. (1998) *Biochem. J. 333*, 139−149.
36. Oki, N., Takahashi, S. I., Hidaka, H., and Conti, M. (2000) *J. Biol. Chem. 275*, 10831−10837.
37. Grange, M., Sette, C., Cuomo, M., Conti, M., Lagarde, M., Prigent, A. F., and Nemoz, G. (2000) *J. Biol. Chem. 275*, 33379−33387.
38. Saldou, N., Obernolte, R., Huber, A., Baecker, P. A., Wilhelm, R., Alvarez, R., Li, B., Xia, L., Callan, O., Su, C., Jarnagin, K., and Shelton, E. R. (1998) *Cell Signal. 10*, 427−440.
39. Zhan, C. G., and Zheng, F. (2001) *J. Am. Chem. Soc. 123*, 2835−2838.

BI010096P